



Lengger, S., Weber, Y., Taylor, K., Berstan, R., Bull, I. D., Mayser, J. P., Leavitt, W., Blewett, J., Pearson, A., & Pancost, R. D. (2021). Determination of the  $\delta^{2}\text{H}$  values of high molecular weight lipids by high-temperature gas chromatography coupled to isotope ratio mass spectrometry. *Rapid Communications in Mass Spectrometry*, 35(4), Article e8983. <https://doi.org/10.1002/rcm.8983>

Peer reviewed version

Link to published version (if available):  
[10.1002/rcm.8983](https://doi.org/10.1002/rcm.8983)

[Link to publication record in Explore Bristol Research](#)  
PDF-document

This is the author accepted manuscript (AAM). The final published version (version of record) is available online via Wiley at <https://doi.org/10.1002/rcm.8983>. Please refer to any applicable terms of use of the publisher.

## University of Bristol - Explore Bristol Research

### General rights

This document is made available in accordance with publisher policies. Please cite only the published version using the reference above. Full terms of use are available: <http://www.bristol.ac.uk/red/research-policy/pure/user-guides/ebr-terms/>



**Determination of the  $\delta^2\text{H}$  values of high molecular weight lipids by high temperature GC coupled to isotope ratio mass spectrometry**

Journal:	<i>Rapid Communications in Mass Spectrometry</i>
Manuscript ID	RCM-20-0242.R1
Wiley - Manuscript type:	Research Article
Date Submitted by the Author:	n/a
Complete List of Authors:	Lengger, Sabine; Plymouth University, School of Geography, Earth and Environmental Science Weber, Yuki; Harvard University, Earth and Planetary Sciences Taylor, Kyle; Isoprime Limited Kopf, Sebastian; University of Colorado Boulder, Department of Geological Sciences Berstan, Robert; Isoprime Limited Bull, Ian; University of Bristol, School of Chemistry Mayser, Jan-Peter; University of Bristol, School of Chemistry Leavitt, William; Dartmouth College Blewett, Jerome; University of Bristol, School of Chemistry Pearson, Ann; Harvard University, Department of Earth and Planetary Sciences Pancost, Rich; University of Bristol
Keywords:	Compound specific isotope analysis, Isotope ratio mass spectrometry, Hydrogen isotopes, Gas chromatography, High molecular weight compounds, High temperature gas chromatography
Abstract:	<p>Rationale: The hydrogen isotopic composition of lipids (<math>\delta^2\text{H}_{\text{lipid}}</math>) is widely used in food science and as a proxy for past hydrological conditions. Determining the <math>\delta^2\text{H}</math> values of large, well-preserved triacylglycerides and other microbial lipids, such as glycerol dialkyl glycerol tetraether (GDGT) lipids, is thus of widespread interest but has so far not been possible due to their low volatility which prohibits analysis by traditional gas chromatography pyrolysis isotope ratio mass spectrometry (GC/P/IRMS).</p> <p>Methods: We determined the <math>\delta^2\text{H}</math> values of large, polar molecules and applied high temperature gas chromatography (HTGC) methods on a modified GC-/P/IRMS system. The system used a high temperature 7 m GC column, and a glass Y-splitter for low thermal mass. Methods were validated using authentic standards of large, functionalised molecules (triacylglycerides, TG), purified standards of GDGTs, and compared to <math>\delta^2\text{H}</math> values determined by elemental analyser pyrolysis isotope ratio mass spectrometry (HTEA/IRMS); and subsequently applied to the analysis of GDGTs in a sample from a methane seep and a Welsh peat.</p> <p>Results: <math>\delta^2\text{H}</math> values of TGs agreed within error between GC/P/IRMS and HTEA/IRMS, with GC/P/IRMS showing larger errors. Archaeal lipid</p>

1  
2  
3  
4  
5  
6  
7  
8  
9  
10  
11  
12  
13  
14  
15  
16  
17  
18  
19  
20  
21  
22  
23  
24  
25  
26  
27  
28  
29  
30  
31  
32  
33  
34  
35  
36  
37  
38  
39  
40  
41  
42  
43  
44  
45  
46  
47  
48  
49  
50  
51  
52  
53  
54  
55  
56  
57  
58  
59  
60

	<p>GDGTs with up to three cyclisations could be analysed: <math>\delta 2H</math> values were not significantly different between methods with standard deviations of 5 to 6 ‰. When environmental samples were analysed, <math>\delta 2H</math> values of isoGDGTs were 50 ‰ more negative than those of terrestrial brGDGTs. Conclusions: Our results indicate that the high temperature GC/P/IRMS (HTGC/P/IRMS) method developed here is appropriate to determine the <math>\delta 2H</math> values of TGs, GDGTs with up to two cyclisations, and potentially other high molecular weight compounds. The methodology will widen the current analytical window for biomarker and food light stable isotope analyses. Moreover, our initial measurements suggest that bacterial and archaeal GDGT <math>\delta 2H</math> values can record environmental and ecological conditions.</p>

SCHOLARONE™  
Manuscripts

1  
2  
3 1 **Determination of the  $\delta^2\text{H}$  values of high molecular weight lipids by high temperature**

4  
5 2 **GC coupled to isotope ratio mass spectrometry**

6  
7  
8 3 Sabine K. Lengger<sup>1,2,\*</sup>, Yuki Weber<sup>3</sup>, Kyle W.R. Taylor<sup>4</sup>, Sebastian H. Kopf<sup>5</sup>, Robert Berstan<sup>4</sup>,

9  
10 4 Ian D. Bull<sup>1</sup>, Jan-Peter Mayser<sup>1</sup>, William D. Leavitt<sup>6</sup>, Jerome Blewett<sup>1</sup>, Ann Pearson<sup>3</sup> and

11  
12 5 Richard D. Pancost<sup>1,7</sup>

13  
14  
15 6 1 Organic Geochemistry Unit, School of Chemistry, University of Bristol, Cantock's Close,

16  
17 7 Bristol BS81TS, UK

18  
19  
20 8 2 Biogeochemistry Research Centre, School of Geography, Earth and Environmental

21  
22 9 Science, University of Plymouth, Drake Circus, Plymouth PL48AA, UK

23  
24  
25 10 3 Department of Earth and Planetary Sciences, Harvard University, 20 Oxford St,

26  
27 11 Cambridge, MA 02138, USA

28  
29  
30 12 4 Elementar UK Ltd., Earl Road, Cheadle Hulme, Stockport, SK8 6PT, UK

31  
32  
33 13 5 Department of Geological Sciences, University of Colorado Boulder, Boulder, CO, USA

34  
35 14 6 Department of Earth Science, Department of Chemistry, Department of Biological

36  
37 15 Sciences, Dartmouth College, Hanover, NH, USA

38  
39  
40 16 7 School of Earth Sciences and Cabot Institute for the Environment, University of Bristol,

41  
42 17 Queens Road, Bristol BS81RL, UK

43  
44  
45 18 \* corresponding author: [sabine.lengger@plymouth.ac.uk](mailto:sabine.lengger@plymouth.ac.uk)

46  
47  
48 19  
49 20 **Abstract**

50  
51  
52 21 Rationale: The hydrogen isotopic composition of lipids ( $\delta^2\text{H}_{\text{lipid}}$ ) is widely used in food

53  
54 22 science and as a proxy for past hydrological conditions. Determining the  $\delta^2\text{H}$  values of large,

55  
56 23 well-preserved triacylglycerides and other microbial lipids, such as glycerol dialkyl glycerol

57  
58 24 tetraether (GDGT) lipids, is thus of widespread interest but has so far not been possible due

59  
60

1  
2  
3 25 to their low volatility which prohibits analysis by traditional gas chromatography pyrolysis  
4  
5 26 isotope ratio mass spectrometry (GC/P/IRMS).  
6  
7

8 27 Methods: We determined the  $\delta^2\text{H}$  values of large, polar molecules and applied high  
9  
10 28 temperature gas chromatography (HTGC) methods on a modified GC-/P/IRMS system. The  
11  
12 29 system used a high temperature 7 m GC column, and a glass Y-splitter for low thermal  
13  
14 30 mass. Methods were validated using authentic standards of large, functionalised molecules  
15  
16 31 (triacylglycerides, TG), purified standards of GDGTs, and compared to  $\delta^2\text{H}$  values  
17  
18 32 determined by elemental analyser pyrolysis isotope ratio mass spectrometry (HTEA/IRMS);  
19  
20 33 and subsequently applied to the analysis of GDGTs in a sample from a methane seep and a  
21  
22 34 Welsh peat.  
23  
24

25 35 Results:  $\delta^2\text{H}$  values of TGs agreed within error between GC/P/IRMS and HTEA/IRMS , with  
26  
27 36 GC/P/IRMS showing larger errors. Archaeal lipid GDGTs with up to three cyclisations could  
28  
29 37 be analysed:  $\delta^2\text{H}$  values were not significantly different between methods with standard  
30  
31 38 deviations of 5 to 6 ‰. When environmental samples were analysed,  $\delta^2\text{H}$  values of  
32  
33 39 isoGDGTs were 50 ‰ more negative than those of terrestrial brGDGTs.  
34  
35

36 40 Conclusions: Our results indicate that the high temperature GC/P/IRMS (HTGC/P/IRMS)  
37  
38 41 method developed here is appropriate to determine the  $\delta^2\text{H}$  values of TGs, GDGTs with up  
39  
40 42 to two cyclisations, and potentially other high molecular weight compounds. The  
41  
42 43 methodology will widen the current analytical window for biomarker and food light stable  
43  
44 44 isotope analyses. Moreover, our initial measurements suggest that bacterial and archaeal  
45  
46 45 GDGT  $\delta^2\text{H}$  values can record environmental and ecological conditions.  
47  
48  
49

50 46  
51  
52  
53  
54  
55  
56  
57  
58  
59  
60

## 47 Introduction

48 The stable hydrogen isotopic composition ( $\delta^2\text{H}$  values) of water varies systematically across  
49 the globe <sup>1-3</sup>. The  $\delta^2\text{H}$  values of biological molecules, in turn, are dependent on the  $\delta^2\text{H}$  of  
50 the  $\text{H}_2\text{O}$  available to the producing organism (source water), overprinted by biochemical  
51 processes. The  $\delta^2\text{H}$  values of bulk organic matter and individual compounds are used  
52 across a range of disciplines, e.g., in ecology and biology to trace animal migration patterns  
53 and food webs <sup>4,5</sup>, in forensic science to identify geographical origins of victims or suspects <sup>6</sup>,  
54 and in food science to determine the provenance of products such as honey <sup>7</sup>, milk <sup>8</sup>, and  
55 meat <sup>9</sup>. The determination of  $\delta^2\text{H}$  values has also resulted in substantial discoveries in  
56 archaeology, such as the earliest horse milking <sup>10</sup>, or manuring practices <sup>11</sup>, and has  
57 improved our understanding of past environments and precipitation regimes <sup>12-14</sup>.

58 The  $\delta^2\text{H}$  values of individual lipid biomarkers are particularly useful in paleoenvironmental  
59 studies. In particular, the correlation of lipid  $\delta^2\text{H}$  with source water  $\delta^2\text{H}$  has been widely  
60 documented <sup>12,15,16</sup>, such that leaf waxes are now widely used to reconstruct past  
61 hydrological conditions <sup>12,16-18</sup>. Long-chain *n*-alkanes and other alkanes are often used in this  
62 endeavour because they are—due to their relatively high pKa (~ 50)—less susceptible to  
63 hydrogen exchange than functionalized compound classes commonly found in soils and  
64 sediments. However, a wide range of sedimentary lipids have been analysed for their stable  
65 hydrogen isotopic composition, including *n*-alkanes, fatty acids, alkenones, and, to a lesser  
66 extent, sterols and hopanols <sup>19-23</sup>.

67 The routine and rapid compound-specific  $\delta^2\text{H}$  value determination of biomarkers (as  
68 opposed to labour intensive approaches requiring compound isolation and purification)  
69 requires the application of gas chromatography, coupled to an on-line reactor containing  
70 active graphite, converting individual organic compounds into graphite, CO and  $\text{H}_2$  <sup>21,24-27</sup>.  
71 The produced gas is introduced into an isotope ratio mass spectrometer monitoring  $m/z$  2  
72 ( $^1\text{H}-^1\text{H}$ ) and 3 ( $^1\text{H}-^2\text{H}$ ). This setup requires analytes to be GC-amenable <sup>28</sup>, limiting analyses  
73 to compounds of a molecular weight and polarity low enough to elute at a typical maximum

1  
2  
3 74 capillary column operating temperature of 320 °C. Therefore, only very few larger  
4  
5 75 compounds (eluting later than a C<sub>36</sub> *n*-alkane on an apolar stationary phase) have had their  
6  
7 76 δ<sup>2</sup>H values successfully determined. Existing measurements were achieved by implementing  
8  
9 77 long isothermal holds at 320 °C but only with highly purified and <sup>2</sup>H-labelled compounds <sup>29</sup>,  
10  
11 78 due to the low GC resolution and δ<sup>2</sup>H precision associated with this methodology.

12  
13  
14 79 However, the δ<sup>2</sup>H values of large and/or polar compounds can be of significant interest. For  
15  
16 80 example, the origin of vegetable oils and milk products can be constrained <sup>30–32</sup> with greater  
17  
18 81 specificity when isotopic fingerprinting is based on individual fatty acids instead of bulk  
19  
20 82 organics <sup>33,34</sup>. Moreover, determining the δ<sup>2</sup>H values of intact triacylglycerides (TG, Suppl.  
21  
22 83 Fig. 1A), instead of hydrolysed and derivatised fatty acids, could have many benefits such as  
23  
24 84 eliminating derivatisation biases and increased specificity. TG are routinely characterised in  
25  
26 85 food forensics by high temperature gas chromatography (HTGC<sup>35–37</sup>), but their <sup>2</sup>H signatures  
27  
28 86 are yet to be exploited. Another potential application arises from very long-chain *n*-alkanes  
29  
30 87 that are major constituents of crude oil; their δ<sup>2</sup>H values could be used to assess source rock  
31  
32 88 potential<sup>17,18,38,39</sup>, or for correlating different oils and source rocks <sup>38,40</sup>.

33  
34  
35  
36 89 A third suite of applications centres on glycerol dialkyl glycerol tetraether lipids (GDGTs,  
37  
38 90 Suppl. Fig. 1BC), derived from both Archaea and Bacteria and of wide interest in  
39  
40 91 geochemistry. These membrane lipids are frequently used in proxies for paleotemperature  
41  
42 92 and other environmental variables <sup>41</sup>. In many sedimentary archives, GDGTs are of mixed  
43  
44 93 origins (e.g. <sup>42,43</sup>), and their δ<sup>2</sup>H values could thus be used to distinguish terrigenous from in  
45  
46 94 situ-produced GDGTs, for example in marine sediments. This would substantially improve  
47  
48 95 the application of these GDGT-based proxies. Moreover, in single-source environments, the  
49  
50 96 hydrogen isotopic composition of GDGTs could serve as a paleohydrological proxy, enabling  
51  
52 97 reconstruction of salinity, elevation, or precipitation. More recently, it has been shown that  
53  
54 98 δ<sup>2</sup>H values of bacterial lipids document the metabolic state of the source organisms,  
55  
56 99 potentially representing another application in biogeochemical investigations <sup>44</sup>, and this  
57  
58 100 method will allow to extend such investigations to Archaea.

1  
2  
3 101 In order to determine the stable isotopic composition of some of these large molecules, they  
4  
5 102 are often subjected to chemical degradation, and only fragments (mostly aliphatic moieties)  
6  
7 103 that are more GC-amenable than the parent molecule are analysed by GC/IRMS. For TGs,  
8  
9 104 this involves acid methanolysis<sup>45</sup>. For GDGTs, this involves ether cleavage, followed by  
10  
11 105 reduction<sup>46–51</sup>, often including laborious preparative HPLC steps for cleaning and  
12  
13 106 preconcentration<sup>52</sup>. Aside from being labour intensive, such procedures under acidic  
14  
15 107 conditions could result in hydrogen exchange.

16  
17  
18 108 However, recently, HTGC methods for more direct analysis of these compounds have been  
19  
20 109 developed; identification and quantification of GDGTs has been achieved employing HTGC  
21  
22 110 coupled to time-of-flight mass spectrometry (HTGC/TOFMS) and flame ionisation detection  
23  
24 111 (HTGC/FID<sup>53,54</sup>). Here, we develop these methods further and demonstrate  $\delta^2\text{H}$  analysis of  
25  
26 112 polar and high molecular weight compounds by HTGC coupled to pyrolysis isotope ratio  
27  
28 113 mass spectrometry (HTGC/P/IRMS). We compare the values of purchased, authentic  
29  
30 114 standards (TGs), and purified standards (GDGTs) determined by elemental analyser  
31  
32 115 pyrolysis isotope ratio mass spectrometry (HTEA/IRMS) with the values determined by  
33  
34 116 HTGC/P/IRMS. We then report the  $\delta^2\text{H}$  values of GDGTs in a number of environmental  
35  
36 117 samples.

## 37 38 39 40 118 **Experimental**

### 41 42 43 119 *Standards and environmental samples*

44  
45 120 Triacylglyceride [TG; trimyristin (TG 42:0), tripalmitin (TG 48:0), and tristearin (TG 54:0)] and  
46  
47 121 *n*-alkane standards were purchased from Sigma Aldrich (Gillingham, UK). isoGDGT-2 and  
48  
49 122 isoGDGT-3 standards were purified from biomass of *Sulfolobus solfataricus* (DSM 1616),  
50  
51 123 which was grown in two batches (2 L each) of modified Allen medium<sup>55</sup> using water with a  
52  
53 124  $\delta^2\text{H}$  value of  $-55.0 \pm 0.2$  ‰. Each batch was inoculated with 20 mL of a late log-phase  
54  
55  
56  
57  
58  
59  
60 125 culture, incubated aerobically at 76 °C with agitation at 200 RPM, and harvested in mid-log



1  
2  
3  
4 126 phase at an optical density of 0.442 (600 nm). Cells were collected by centrifugation at 4 °C,  
5  
6  
7 127 frozen in liquid nitrogen, and freeze-dried. 0.5 g of the freeze-dried cell pellet was subjected  
8  
9  
10 128 to acid hydrolysis in 5 mL of 1.5 N methanolic HCl (10 % H<sub>2</sub>O made from 37% HCl) for 3  
11  
12  
13 129 hours at 70°C, and lipids were extracted by ultrasonication in dichloromethane:methanol  
14  
15  
16 130 (1:1; v/v) as previously described<sup>56</sup>. The total lipid extract (TLE) was dried under a stream of  
17  
18  
19 131 N<sub>2</sub>, dissolved in 1 mL of *n*-hexane: isopropanol (97:3; v/v), and filtered through a 0.45 µm  
20  
21  
22 132 PTFE filter.

23  
24  
25  
26 133 To produce purified standards for both HTEA/IRMS, and for GC/P/IRMS, individual  
27  
28 134 isoprenoidal GDGTs containing 2 and 3 cyclopentyl moieties (isoGDGT-2 and isoGDGT-3)  
29  
30 135 were isolated by preparative normal phase (NP) high-performance liquid chromatography  
31  
32 136 (HPLC). To this end, aliquots (25 µL) of the filtered TLE were injected onto an Agilent 1100  
33  
34 137 HPLC system fitted with an Econosphere NH<sub>2</sub> column (250 × 10 mm, 10 µm; Grace/Alltech).  
35  
36 138 GDGTs were eluted isocratically with a solvent mixture of 1.35 % isopropanol (IPA) in  
37  
38 139 *n*-hexane at a flow rate of 1 mL min<sup>-1</sup> for 45 min, and the column was cleaned with 16 % IPA  
39  
40 140 for 12 min and re-equilibrated to initial conditions for 13 min after every run. GDGTs were  
41  
42 141 recovered by time-based fraction collection, according to the elution times determined by  
43  
44 142 atmospheric pressure chemical ionisation-mass spectrometry (APCIMS) using an Agilent  
45  
46 143 1100 MSD quadrupole mass spectrometer (Agilent Technologies, Cheshire, UK)<sup>57</sup>. The  
47  
48 144 collected fractions were analysed by flow injection analysis-APCIMS on the same  
49  
50 145 instrument, and subsequently pooled by compound. The purity of each isolated GDGT was  
51  
52 146 >97 % as assessed by NP and reverse phase HPLC/APCIMS analysis of the combined  
53  
54 147 fractions<sup>58</sup>, scanning the range *m/z* of 350–1350.  
55  
56  
57  
58  
59  
60

1  
2  
3 148 Environmental samples analysed by GC/P/IRMS included a sediment sample from a marine  
4  
5 149 methane seep, and a sample from a Welsh peat<sup>53</sup>. In order to improve gas chromatographic  
6  
7 150 performance, GDGTs were purified prior to HTGC/P/IRMS. The Welsh peat extract was  
8  
9 151 passed over a column containing 130-270 mesh silica (pore size 60 Å 288608, Sigma  
10  
11 152 Aldrich, Gillingham, UK) conditioned in methanol, using two column volumes of each  
12  
13 153 hexane, ethylacetate/hexane 1:9 (v/v), 25:75, 50:50, pure ethylacetate, and methanol.  
14  
15 154 Concentrations of GDGTs in the fractions were confirmed by adding triglyceride  
16  
17 155 quantification standards and analysis by HTGC/FID<sup>53</sup>. All fractions containing GDGTs  
18  
19 156 (Suppl. Fig. 2) were combined to avoid any isotope fractionation which may have occurred  
20  
21 157 during column chromatography.  
22  
23  
24

#### 25 158 *<sup>2</sup>H analysis by HTEA/IRMS*

26  
27  
28

29 159 The <sup>2</sup>H/<sup>1</sup>H ratios of the triacylglycerides (TGs) and C<sub>50</sub> and C<sub>60</sub> *n*-alkanes were analysed  
30  
31 160 via HTEA/IRMS at Elementar UK Ltd (EUK; Stockport, UK) and University of Colorado (CUB;  
32  
33 161 Boulder, USA). CUB also analysed GDGTs. CUB performed HTEA/IRMS on a Flash HT Plus  
34  
35 162 elemental analyser at 1450 °C with zero blank autosampler coupled to a Delta V Plus IRMS  
36  
37 163 via ConFlo-IV Interface (both Thermo Fisher Scientific, Waltham, MA, USA). At EUK,  
38  
39 164 HTEA/IRMS measurements were performed using a Geovision, which comprised a vario  
40  
41 165 PYRO cube elemental analyser coupled to an isoprime vision IRMS (both EUK). Both  
42  
43 166 laboratories measured samples using glassy carbon reactors in oxygen-free environments,  
44  
45 167 and performed multipoint calibrations using reference materials provided by Arndt  
46  
47 168 Schimmelmann (Indiana University, Bloomington, IN, USA) to normalise the measured δ<sup>2</sup>H  
48  
49  
50  
51  
52  
53  
54  
55  
56  
57  
58  
59  
60

1  
2  
3  
4 169 values against the international reference Vienna Standard Mean Ocean Water (VSMOW).  
5  
6  
7 170 CUB calibrated using 5 $\alpha$ -androstane #3 ( $-293.2 \pm 1.0 \text{ ‰}$ ), eicosanoic acid methyl ester #Z1 /  
8  
9  
10 171 USGS 70 ( $-183.9 \pm 1.4 \text{ ‰}$ ), and eicosanoic acid methyl ester #Z2 / USGS 71 ( $-4.9 \pm 1.0 \text{ ‰}$ ),  
11  
12  
13 172 and EUK calibrated using tetracosane #1:  $-53.0 \pm 1.6 \text{ ‰}$ , pentacosane #4:  $-263.6 \pm 2.2 \text{ ‰}$  and  
14  
15  
16 173 heptacosane #3:  $-172.80 \pm 1.6 \text{ ‰}$ , and a standard provided by the International Atomic Energy  
17  
18 174 Agency, Vienna (IAEA CH-7:  $-100.2 \pm 1.0 \text{ ‰}$ ). Across both labs, the standard deviation (SD)  
19  
20 175 of triplicate sample analyses was typically  $< \pm 0.75 \text{ ‰}$ .  
21  
22  
23 176 Because the oxygen-bound H atoms of the GDGTs' hydroxyl moieties are easily exchanged,  
24  
25  
26 177 the  $^2\text{H}$  content at these positions may have been altered during solvent  
27  
28  
29  
30 178 extraction/evaporation. We therefore vapour-equilibrated the dried GDGT fractions with local  
31  
32  
33 179 deionised water ( $-121.8 \pm 1.3 \text{ ‰}$ ) before analysis (24 h at  $25 \text{ }^\circ\text{C}$ ). GDGT fractions were then  
34  
35  
36 180 dissolved in ethyl acetate at  $\sim 10 \text{ } \mu\text{g } \mu\text{L}^{-1}$  and  $10 \text{ } \mu\text{L}$  aliquots were pipetted into combusted  
37  
38  
39 181 ( $450 \text{ }^\circ\text{C}$ , 10 h) silver capsules (4x6 mm), which were pre-loaded with small discs ( $d = 4 \text{ mm}$ )  
40  
41  
42 182 of combusted glass fibre filters (Whatman GF/F) as a solvent adsorbent. The solvent was  
43  
44  
45  
46 183 then completely evaporated in a closed chamber continuously purged with  $\text{N}_2$  (30 min at  
47  
48  
49 184  $\sim 30 \text{ mL min}^{-1}$ ). Analysis by HTEA/IRMS was then conducted as described above.  
50  
51  
52  
53 185 To test for the efficiency of the vapour equilibration, a synthetic diglycerol-trialkyl-tetraether  
54  
55  
56 186 ( $\text{C}_{46}$ -GTGT; Patwardhan and Thompson, 1999) was exposed to vapour of both  $^2\text{H}$ -enriched  
57  
58  
59 187 water (7 atom %  $^2\text{H}$ ) and local deionised water (24 h at  $25 \text{ }^\circ\text{C}$ ). Exposure to  $^2\text{H}$ -enriched  
60

1  
2  
3  
4 188 water vapour increased the  $^2\text{H}$  content of the molecule by 0.1 atom % (from 0.014 to  
5  
6  
7 189 0.113 atom % relative to total H), corresponding to a  $^2\text{H}$  content of  $\sim 5$  atom % at the OH  
8  
9  
10 190 positions after exposure (assuming all exchange is localised to the hydroxyl moieties).  
11  
12  
13 191 Exposure to natural water vapor, however, did not lead to a change in  $\delta^2\text{H}$  within analytical  
14  
15  
16 192 precision of the measurement. The induced  $^2\text{H}$  content at the OH positions decreased again  
17  
18  
19 193 to a  $^2\text{H}$  content of  $\sim 2$  atom % at the OH-positions after a 12 h exposure to ambient lab air.  
20  
21  
22  
23 194 Together this indicates that OH-bound H of diglycerol tetraethers is readily exchanged with  
24  
25  
26 195 ambient water vapor, and any  $^2\text{H}$  enrichment resulting from the evaporation of OH-  
27  
28  
29 196 containing solvents (e.g. methanol) was likely diminished either by spontaneous re-  
30  
31  
32 197 equilibration with ambient air, or by the latest through 24 h exposure to natural water vapor  
33  
34  
35 198 in a desiccator as described above.

#### 199 *$\delta^2\text{H}$ value determination by high-temperature GC/P/IRMS*

200 Before analysis by HTGC/IRMS, fractions containing GDGTs and the sample from the Black  
201 Sea methane seep were dissolved in 50  $\mu\text{L}$  pyridine and derivatised to trimethylsilylethers  
202 with 50  $\mu\text{L}$  99% N,O-Bis(trimethylsilyl)trifluoroacetamide (BSTFA), 1% trimethylchlorosilane  
203 (TMCS), for one hour at 70  $^\circ\text{C}$ . The  $\delta^2\text{H}$  value of the TMS moieties used to derivatise the  
204 hydroxyl-groups ( $\delta^2\text{H}_{\text{TMS}}$ ) was determined by derivatisation of sodium palmitate of a known  
205  $\delta^2\text{H}$  ( $\delta^2\text{H}_P$ , -239.10 ‰), and analysis by GC/IRMS to yield the values of derivatised palmitate  
206  $\delta^2\text{H}_{\text{TMS}}$ , as -82.35 ‰ according to Eqn. 1. The use of  $\delta$ -values in this specific case is  
207 possible and recommended (natural abundance ranges), when larger differences are  
208 present, D/H ratios must be used.

$$\delta^2 H_{TMS} = \frac{\delta^2 H_{TMSP} \cdot 40 - \delta^2 H_P \cdot 31}{9} \quad (Eqn 1)$$

Values of derivatised GDGTs  $\delta^2 H_{meas}$  were corrected by mass balance to give  $\delta^2 H_{GDGT}$  with  $n$  representing the number of non-exchangeable hydrogens of the compounds and  $k$  the number of TMS groups added (1 for archaeol, 2 for GDGTs and hydroxyarchaeol; Eqn. 2).

$$\delta^2 H_{GDGT} = \frac{\delta^2 H_{meas}(n + k \cdot 9)}{n} - \frac{k \cdot 9 \cdot \delta^2 H_{TMS}}{n} \quad (Eqn 2)$$

This was combined into Eqn. 3.

$$\delta^2 H_{GDGT} = \frac{\delta^2 H_{meas}(n + k \cdot 9)}{n} - \frac{k \cdot 40 \cdot \delta^2 H_{TMSP}}{n} + \frac{k \cdot 31 \cdot \delta^2 H_P}{n} \quad (Eqn 3)$$

Errors of  $\delta^2 H_{meas}$  were determined according to error propagation laws:

$$\sigma_{\delta^2 H_{GDGT}}^2 = \sigma_{\delta^2 H_{meas}}^2 \cdot \left(\frac{n + k \cdot 9}{n}\right)^2 + \sigma_{\delta^2 H_{TMSP}}^2 \cdot \left(\frac{k \cdot 40}{n}\right)^2 + \sigma_{\delta^2 H_P}^2 \cdot \left(\frac{k \cdot 31}{n}\right)^2 \quad (Eqn 4)$$

Samples were screened by HTGC/FID as described by Lengger et al.<sup>53</sup> before they were analysed by an Elementar isoprime vision HTGC/P/IRMS (Elementar UK Ltd., Cheadle, UK). The instrument comprised an Agilent 7890B GC fitted with an on-column injector, linked to a GC5 interface (maintained at 380 °C) and a hollow ceramic reactor, in which a stripped transfer line (Zebron Z-Guard high temperature guard column, 0.25 mm ID, Phenomenex Ltd., Aschaffenburg, Germany) was inserted carrying analytes from the GC, enabling pyrolysis at 1450 °C. A PTV injector was not available on this instrument, but was observed to inhibit elution of GDGTs in separate investigations (data not shown). Ferrules used to connect the ceramic furnace and GC-column, as well as the sample line He used as an additional carrier in the HTGC/P/IRMS system, were 100% graphite. Ion beams at  $m/z$  2 and 3 were monitored via an isoprime vision mass spectrometer. The  $H_3^+$  factor was determined

1  
2  
3 234 daily or at least every 4 runs. Compounds were injected in ethylacetate (1  $\mu\text{L}$ ) and separated  
4  
5 235 on a Zebron ZB-5HT analytical column (7 m  $\times$  0.25 mm  $\times$  0.25  $\mu\text{m}$ , Phenomenex Ltd.,  
6  
7 236 Aschaffenburg, Germany) with high-temperature resistant polyimide coating, which was  
8  
9 237 fitted to a transfer line (Zebron Z-Guard Hi-Temp guard column 0.25 mm ID, Phenomenex  
10  
11 238 Ltd., Aschaffenburg, Germany) that was inserted directly into the reactor (with the reactor-  
12  
13 239 facing side thermally stripped of polyimide coating), and an exhaust to allow diversion of the  
14  
15 240 solvent peak to waste via a glass Y-splitter, in which columns were fixed with high  
16  
17 241 temperature resin (Phenomenex Ltd., Aschaffenburg, Germany). He was used as a carrier  
18  
19 242 gas at a flow rate of 2.2  $\text{mL min}^{-1}$ , and the oven was programmed as follows: 1 min hold at  
20  
21 243 70  $^{\circ}\text{C}$ , increase by 10  $^{\circ}\text{C min}^{-1}$  to 350  $^{\circ}\text{C}$ , followed by an increase at 3  $^{\circ}\text{C min}^{-1}$  to 400  $^{\circ}\text{C}$  (10  
22  
23 244 min hold). Results were calibrated using a mixture of *n*-alkanes (B3, A. Schimmelmann,  
24  
25 245 Indiana University, Bloomington, IN, USA) according to Sessions et al.<sup>21,60</sup>, which was  
26  
27 246 injected at least every four analyses (RMS detailed in Tab. S1), and analysed using a He  
28  
29 247 flow of 1  $\text{mL min}^{-1}$ , with a different temperature program (injection at 50  $^{\circ}\text{C}$  held for 1 min  
30  
31 248 followed by an increase of 10  $^{\circ}\text{C min}^{-1}$  to 300  $^{\circ}\text{C}$  and a 10 min hold). Resultant calibrated  $\delta^2\text{H}$   
32  
33 249 values were calculated based on the derived linear regression. Root mean standard errors of  
34  
35 250 normalised values of the *n*-alkane mixture were typically between 4 and 6 ‰, and never  
36  
37 251 exceeded 10 ‰. Data was processed using ionOS stable isotope data processing software  
38  
39 252 (Elementar UK Ltd., UK), using an automated multi-point linearisation based on the certified  
40  
41 253 values of the 15 individual *n*-alkanes comprising the B3 standard.  
42  
43  
44  
45

46 254 The fractionation factor  $\varepsilon_{\text{H}_2\text{O}/\text{GDGT}}$  was determined from the  $\delta^2\text{H}_{\text{H}_2\text{O}}$  and the  $\delta^2\text{H}_{\text{GDGT}}$  (Eqn. 5).  
47  
48

49 255 
$$\varepsilon_{\text{GDGT}/\text{H}_2\text{O}} = \left( \frac{\delta_{\text{GDGT}} + 1}{\delta_{\text{H}_2\text{O}} + 1} - 1 \right)$$

50  
51  
52  
53 256 (Eqn. 5)  
54  
55

## 56 257 **Results and discussion**

### 57 58 258 *Chromatographic method*

59  
60

1  
2  
3 259 The modifications of the GC/IRMS instrumentation enabled operating temperatures of up to  
4  
5 260 400 °C. Utilisation of a 7-m column and on-column injection (as previously discussed <sup>53</sup>)  
6  
7 261 enabled elution of isoGDGTs up to GDGT-3, as well as acceptable values for the B3  
8  
9 262 standard. The GC/P/IRMS setup required a polyimide-coated column rather than the metal  
10  
11 263 column commonly employed in HTGC-methodologies, as this allowed flow diversion via a  
12  
13 264 glass Y-splitter in which the column was secured using high temperature resin (no other  
14  
15 265 modifications to the standard Elementar flow diversion system were made). The glass Y-  
16  
17 266 splitter ensured minimal thermal mass. The small ID of the ceramic reactor and insertion of  
18  
19 267 the transfer line close to the pyrolysis site, and of contact with any metal surfaces (glass Y-  
20  
21 268 splitter instead of metal valve, silicon transfer to pyrolysis site in ceramic reactor), have likely  
22  
23 269 contributed to avoid the peak broadening and fronting often observed in GC/P/IRMS.  
24  
25 270 Furthermore, the pneumatically operated heart-cut valve enabling diversion of the solvent  
26  
27 271 away from the furnace reactor was moved to a location outside of the GC-oven in order to  
28  
29 272 avoid potential leaks associated with the high temperatures. Extended (> 10 min) high  
30  
31 273 temperature (> 400 °C) isothermals such as used successfully with metal columns to  
32  
33 274 analyse isoGDGTs by HTGC/FID and HTGC-TOFMS <sup>53</sup>, could not be employed to elute  
34  
35 275 isoGDGTs in analogous HTGC/P/IRMS analyses due to the comparatively lower stability of  
36  
37 276 the polyimide-coated columns at these temperatures.

38  
39  
40  
41 277 The unusual HTGC configuration, with a short 7 m column, high flow, and on-column  
42  
43 278 injector, was tested by analysing a mixture of 15 *n*-alkanes: the so-called Indiana B-standard  
44  
45 279 mix routinely used for standardisation of GC/P/IRMS results. Baseline separation of  
46  
47 280 individual *n*-alkane peaks and acceptable root mean square errors were achieved with this  
48  
49 281 method (Fig. 1A): this standard was subsequently used for quality control and isotope  
50  
51 282 calibration. Root mean square error (RMSE) and linearisation equations for all analyses of  
52  
53 283 the standards are given in Supplementary Fig. 3 and Table 1, with linearisation applied to  
54  
55 284 the samples based on the most contemporary analysis of the standard. RMSE for all  
56  
57 285 accepted analyses were always below 10 ‰: whenever 10 ‰ was exceeded, inlet maintenance  
58  
59  
60

1  
2  
3 286 or column changes were performed. An *n*-alkane standard containing higher molecular  
4  
5 287 weight compounds (up to C<sub>60</sub>, Fig. 1B), a mixture of triacylglycerides (Fig. 1C), a seep  
6  
7 288 sample containing GDGT-0, -1, -2, and -3, and the two GDGT standards (GDGT-2 and -3)  
8  
9 289 (Fig. 1D) were analysed and chromatograms were similar to previous results employing  
10  
11 290 HTGC/FID and a 7 m column<sup>53</sup>. The brGDGTs eluted earlier than isoGDGTs (cf.<sup>53</sup>). The  
12  
13 291 unusual HTGC configuration, with a short 7 m column, high flow, and on-column injector,  
14  
15 292 was tested by analysing a mixture of 15 *n*-alkanes: the so-called Indiana B-standard mix  
16  
17 293 routinely used for standardisation of GC/IRMS results. Baseline separation of individual *n*-  
18  
19 294 alkane peaks and acceptable root mean square errors were achieved with this method (Fig.  
20  
21 295 1A). The Indiana B3 standard was subsequently used for quality control and isotope  
22  
23 296 calibration. Root mean square error (RMSE) and linearisation equations for all analyses of  
24  
25 297 the standards are given in Table 1 and Supplementary Fig. 3, with linearisation applied to  
26  
27 298 the samples based on the most contemporary analysis of the standard. RMSE for all  
28  
29 299 accepted analyses were always below 10 ‰: whenever 10 was exceeded, inlet maintenance  
30  
31 300 or column changes were performed. An *n*-alkane standard containing higher molecular  
32  
33 301 weight compounds (up to C<sub>60</sub>, Fig. 1B), a mixture of triacylglycerides (Fig. 1C), a seep  
34  
35 302 sample containing GDGT-0, -1, -2, and -3, and the two GDGT standards (GDGT-2 and -3)  
36  
37 303 (Fig. 1D) were analysed and chromatograms were similar to previous results employing  
38  
39 304 HTGC/FID and a 7 m column<sup>53</sup>. The brGDGTs eluted earlier than isoGDGTs (cf.<sup>53</sup>).  
40  
41  
42  
43

#### 305 *Accuracy and precision of δ<sup>2</sup>H values of high molecular weight compounds*

44  
45  
46 306 Triacylglyceride (TG) reference compounds and purified GDGT standards were used to test  
47  
48 307 the methodology for accuracy by determining the δ<sup>2</sup>H values of these compounds by  
49  
50 308 HTGC/IRMS at GC temperatures of up to 400 °C as well as by EA-analysis. The prepared  
51  
52 309 isoGDGT-2 and isoGDGT-3 standards were analysed by one laboratory (CU Boulder), while  
53  
54 310 the purchased standards were examined by HTEA/IRMS in two different laboratories (CU  
55  
56 311 Boulder and Elementar UK Ltd). The average δ<sup>2</sup>H values determined for the TGs were within  
57  
58 312 5 ‰ for all analyses (Tab. 1, Fig. 2). HTGC-analysed samples generally yielded δ<sup>2</sup>H values  
59  
60



1  
2  
3 313 between the values determined by the EA analyses. Standard deviations were smaller for  
4  
5 314 the EA methods ( $< 2 \text{ ‰}$ ) than for the HTGC method (9-18 ‰, which represents 2-3× the  
6  
7 315 typical precision of  $\delta^2\text{H}$  value determinations by GC/P/IRMS<sup>61</sup>, and is thus a larger error  
8  
9 316 than expected). Often, precision of GC/P/IRMS measurements is determined using the same  
10  
11 317 concentration, while here, injection concentrations varied. This likely contributed to the high  
12  
13 318 standard deviation, and we investigate this further below. It is expected that further  
14  
15 319 application of this technique – and routine analysis of TGs, as compounds of particular  
16  
17 320 interest to the food industry – will lead to improvements in analytical precision as methods  
18  
19 321 are improved by optimising solvents, injection temperatures, and concentrations. The  $\delta^2\text{H}$   
20  
21 322 values determined for the high molecular weight *n*-alkanes with 50 and 60 carbon atoms  
22  
23 323 (Table 1) were more variable among all methods and laboratories. This was surprising, and  
24  
25 324 possibly a result of insufficient mixing of these large waxy compounds before distribution to  
26  
27 325 other laboratories.

30  
31 326 The  $\delta^2\text{H}$  values of purified GDGTs obtained by HTEA/IRMS and HTGC/IRMS (Tab. 1) were  
32  
33 327 not significantly different for GDGT-2 at a high confidence level (Welsh's t-test,  $df = 2$ ,  $t =$   
34  
35 328 1.32,  $p = 0.32$ ). However, for GDGT-3, which eluted later, the  $\delta^2\text{H}$  value derived by  
36  
37 329 HTGC/IRMS was 9 ‰ higher than the value determined by HTEA/IRMS ( $df = 2$ ,  $t = 3.32$ ,  $p$   
38  
39 330 = 0.080). A high baseline could be a possible cause for this discrepancy. However, ionOS  
40  
41 331 software applies an automated correction. Both GDGTs eluted on an isothermal baseline  
42  
43 332 when samples were injected (Fig. 1D). Another cause could be fractionation due to  
44  
45 333 chromatographic separation, adsorption to cold spots, or thermal decomposition. Another  
46  
47 334 possibility is minor contamination of GDGT-3, resulting in a flawed HTEA/IRMS  
48  
49 335 measurement but not affecting HTGC/P/IRMS measurements; however, this would be  
50  
51 336 surprising as GDGT-2 and GDGT-3 were isolated from the same organism and the  
52  
53 337 HTEA/IRMS results match expectations of similar  $\delta^2\text{H}$  values. The standard deviation of 5 –  
54  
55 338 6 ‰ achieved for purified GDGTs using the HTGC/P/IRMS system is similar to the precision  
56  
57 339 of lower molecular weight compounds on a conventional GC/P/IRMS instrument<sup>61</sup>.

### 340 *Response vs accuracy*

341 Whilst GDGTs are ubiquitous, they are typically only present at ppm to ppb concentrations in  
342 environmental samples such as sediments and soils. In addition, many high molecular  
343 weight compounds are not very soluble in solvents suitable for GC/IRMS, and on-column  
344 injection only allows small amounts of sample to be used. Therefore, only small amounts of  
345 GDGT (ng) were injected for each HTGC/P/IRMS analysis. To assess accuracy in  
346 relationship to signal intensity, different concentrations of the TG standard were tested and  
347 compared to peak heights (Fig. 3). This yielded a response of 0.07 – 0.08 nA per ng H per  
348 compound for  $m/z$  2 (equivalent to 70-80 mV on an IRMS with a  $10^9$  Ohm resistor on the  
349 operational amplifier for the  $m/z$  2 faraday cup). Below ~0.25 nA peak height, values begin to  
350 deviate substantially (by ~20 ‰) from the values measured by HTEA/IRMS, with differences  
351 of up to 400 ‰ when peak heights were around 0.1 nA. We thus excluded peak heights <  
352 0.25 nA, corresponding to less than 3.5 ng H injected on column, from any further analysis.  
353 Typical H amounts required to achieve 3-5 ‰ precision were ~10 ng, translating to  $m/z$  2  
354 peak heights of 0.7 – 0.8 nA.

### 355 *GDGTs in environmental samples and $\epsilon_{H_2O/isoGDGT}$*

356 A sample from a Mediterranean cold seep<sup>53</sup> was analysed, and  $\delta^2H$  values for archaeol,  
357 hydroxyarchaeol, GDGT-1, and GDGT-2 were determined to be  $-245 \pm 7$ ,  $-253 \pm 13$ ,  $-216 \pm$   
358  $15$ , and  $-225 \pm 14$ , respectively ( $n=3$ ; Fig. 1D, Fig. 4). These values show a limited range, as  
359 expected for ether lipids derived from a common archaeal source, and are similar to  
360 published  $\delta^2H$  values of the biphytanes of GDGTs in *Sulfolobus sp.* determined after ether  
361 cleavage ( $-229$  to  $-257$  ‰<sup>46</sup>). However, the values are not identical: the diphytanyl glycerol  
362 diether lipids archaeol and hydroxyarchaeol were  $^2H$ -depleted relative to GDGTs. Though  
363 the difference between the di- and tetraethers is small, and similar to what is commonly  
364 observed between different fatty acids from the same organism<sup>62</sup>, it could potentially reflect  
365 different archaeal origins, given that ANME-2 group Archaea appear to preferentially  
366 produce GDGTs in cold seep settings (e.g., Blumenberg et al., 2004). This would be

1  
2  
3 367 particularly true if the differing source Archaea exhibit different metabolisms (see below). A  
4  
5 368 sample from a Mediterranean cold seep<sup>53</sup> was analysed, and  $\delta^2\text{H}$  values for archaeol,  
6  
7 369 hydroxyarchaeol, GDGT-1, and GDGT-2 were determined to be  $-245 \pm 7$ ,  $-253 \pm 13$ ,  $-216 \pm$   
8  
9 370  $15$ , and  $-225 \pm 14$ , respectively ( $n=3$ ; Fig. 1D, Fig. 4). These values show a limited range, as  
10  
11 371 expected for ether lipids derived from a common archaeal source, and are similar to  
12  
13 372 published  $\delta^2\text{H}$  values of the biphytanes of GDGTs in *Sulfolobus sp.* determined after ether  
14  
15 373 cleavage ( $-229$  to  $-257$  ‰)<sup>46</sup>. However, the values are not identical, with the diphytanyl  
16  
17 374 glycerol diether lipids archaeol and hydroxyarchaeol being  $^2\text{H}$ -depleted relative to GDGTs.  
18  
19 375 The difference is small, and similar to what is commonly observed between different fatty  
20  
21 376 acids from the same organism<sup>62</sup>, however, it could potentially reflect different archaeal  
22  
23 377 origins, given that ANME-2 group Archaea appear to preferentially produce GDGTs in cold  
24  
25 378 seep settings (e.g., Blumenberg et al., 2004). This would be particularly true if the differing  
26  
27 379 source Archaea exhibit different metabolisms (see below).

30  
31 380 The  $\epsilon_{\text{H}_2\text{O}/\text{GDGT}}$  for the *Sulfolobus* cultures used to purify the standards was determined as  
32  
33 381  $-134$  ‰ and was lower than previously reported  $\epsilon_{\text{H}_2\text{O}/\text{GDGT}}$  ( $-213$ ‰ to  $-161$ ‰<sup>46</sup>). The  
34  
35 382 application of this fractionation factor to the environmental iso-GDGTs would result in an  
36  
37 383 unrealistic  $\delta^2\text{H}$  value for the seawater of  $-93$  ‰, suggesting that metabolism, salinity,  
38  
39 384 temperature, and other factors contribute strongly to the extent of fractionation.

40  
41  
42 385 Values of  $\delta^2\text{H}$  of GDGT-0 from the peat (Suppl. Fig. 4) were similar to the isoGDGTs in the  
43  
44 386 seep sample ( $-235 \pm 3$  ‰,  $n = 2$ ), whereas values for brGDGTs (integrated as one peak)  
45  
46 387 were relatively enriched in  $^2\text{H}$  ( $-176 \pm 6$  ‰,  $n = 6$ ). It is possible that the  $^2\text{H}$ -enrichment of  
47  
48 388 brGDGTs relative to co-occurring isoGDGTs could be due to fractionation associated with  
49  
50 389 the biosynthetic pathways for isoprenoidal (isoGDGTs) vs. *n*-acyl lipids (brGDGTs), in which  
51  
52 390 isoprenoidal lipids (which undergo successive hydrogenation) exhibit more  $^2\text{H}$ -depleted  
53  
54 391 signatures<sup>21,64</sup>. However, recently, it has also been shown that the energy and metabolism  
55  
56 392 pathways of source organisms are highly correlated with  $\delta^2\text{H}$  values of their lipids<sup>44,65,66</sup>; it is  
57  
58 393 also thought that NADPH/NADH ratios and transhydrogenases play an important role,  
59  
60

1  
2  
3 394 particularly in anaerobic organisms<sup>67–70</sup>. In general, heterotrophic bacteria consuming TCA-  
4  
5 395 cycle intermediates exhibit  $\delta^2\text{H}$  values similar to or more positive than the source water,  
6  
7 396 heterotrophs assimilating carbohydrates are depleted relative to source water, and  
8  
9 397 photoautotrophic and chemoautotrophic bacteria show the greatest  $^2\text{H}$ -depletion<sup>44</sup>. While  
10  
11 398 Archaea were not examined in this work, some of our results are consistent with the idea  
12  
13 399 that chemoautotrophic archaea are the presumed producers of isoGDGTs in both settings,  
14  
15 400 and heterotrophic bacteria are thought to be the producers of brGDGTs<sup>71</sup>.

16  
17  
18 401 The differences between the peat and seep samples for isoGDGTs are unexpected: As the  
19  
20 402  $\delta^2\text{H}$  of the peat water is likely around  $-52\text{‰}$ <sup>1</sup> – a  $^2\text{H}$  content that is depleted compared to  
21  
22 403 seawater – we expected isoGDGTs from peat to also be depleted in  $^2\text{H}$  relative to GDGTs  
23  
24 404 from marine environments. However, isoGDGTs from peat are up to 10 to 20 ‰ more  $^2\text{H}$ -  
25  
26 405 enriched from peat, invoking a difference in metabolic state between the anaerobic  
27  
28 406 methanogens in peat, and the anaerobic methane oxidising communities in the seep. It  
29  
30 407 could also indicate syntrophy, which has been shown to affect  $^2\text{H}$  values of lipids<sup>68</sup>. These  
31  
32 408 findings speak to the potential of isoGDGT  $\delta^2\text{H}$  analyses in probing microbial ecology and  
33  
34 409 metabolic state, while brGDGTs, which are presumably of heterotrophic bacterial origin in  
35  
36 410 peat settings, could prove useful as proxies for source water  $\delta^2\text{H}$  and hydrology.

37  
38  
39 411 The novel HTGC/P/IRMS method enables the determination of the  $\delta^2\text{H}$  values of  
40  
41 412 compounds with a high molecular weight, including TG and GDGTs, hereby extending the  
42  
43 413 range of analytes for  $\delta^2\text{H}$  value determination. Accuracy and precision are as small as 3 ‰  
44  
45 414 in some cases and comparable to HTEA/IRMS. Our initial measurements suggest that  
46  
47 415 bacterial and archaeal GDGT  $\delta^2\text{H}$  values are likely both related to environmental  
48  
49 416 parameters, and the metabolic and ecological function of the source organisms. Future  
50  
51 417 applications include but are not limited to food forensics, archaeology, oil-source rock  
52  
53 418 correlations, microbial ecology and paleoclimate.

## 54 55 56 57 58 419 **Acknowledgements**

1  
2  
3 420 We would like to thank the Editor, three anonymous reviewers, and A. Sessions for their  
4  
5 421 helpful comments. The authors would like to thank Paul Sutton, Alison Kuhl, Hanna  
6  
7 422 Gruszczynska, Ed Aldred, Xiahong Feng, Alec Cobban, Wolfram Meier-Augenstein, and  
8  
9 423 Michiel Kienhuis for support with measurements, advice, and discussions of techniques. SKL  
10  
11 424 was funded by a Rubicon Grant 825.14.014 from the Netherlands Organisation for Scientific  
12  
13 425 Research (NWO, to SKL). RDP acknowledges support from ERC (Advanced Grant T-GRES,  
14  
15 426 to RDP). AP and YW acknowledge support from the Swiss National Science Foundation  
16  
17 427 (P2BSP2\_168716), and from the Gordon and Betty Moore Foundation and US National  
18  
19 428 Science Foundation (to AP). SHK acknowledges support from the US National Science  
20  
21 429 Foundation. The authors thank the Natural Environment Research Council, UK, for partial  
22  
23 430 funding of the mass spectrometry facilities at Bristol (contract no. R8/H10/63). WDL  
24  
25 431 acknowledges support from the American Chemical Society (PRF 57209-DNI2).  
26  
27  
28  
29 432  
30  
31  
32  
33  
34  
35  
36  
37  
38  
39  
40  
41  
42  
43  
44  
45  
46  
47  
48  
49  
50  
51  
52  
53  
54  
55  
56  
57  
58  
59  
60

**Table 1.**  $\delta^2\text{H}$  values determined by HTEA/IRMS and HTGC/P/IRMS.

	HTEA/IRMS (Elementar)			HTEA/IRMS (CU Boulder)			HTGC/IRMS		
	Mean	St. dev.	N	Mean	St. dev.	N	Mean	St. dev.	N
	[‰ V-SMOW]			[‰ V-SMOW]			[‰ V-SMOW]		
<b>GDGT-2</b>	-	-	-	-181.6	0.4	3	-186	4	3
<b>GDGT-3</b>	-	-	-	-182.6	0.2	3	-173	7	3
<b>C<sub>42</sub>-TG 42:0</b>	-235.0	0.5	4	-238.0	0.7	3	-232	9	9
<b>C<sub>48</sub>-TG 48:0</b>	-219	2	3	-224.1	0.3	3	-223	18	7
<b>C<sub>54</sub>-TG 54:0</b>	-225.9	0.4	4	-228.2	0.7	3	-223	12	7
<b><i>n</i>-C<sub>60</sub> alk</b>	-206	5	3	-214.0	0.4	3	-196	3	3
<b><i>n</i>-C<sub>50</sub> alk</b>	-199.29	0.02	4	-202.05	0.06	3	-188	3	3

## References

1. Bowen GJ, Revenaugh J. Interpolating the isotopic composition of modern meteoric precipitation. *Water Resour Res.* 2003;39(10). doi:10.1029/2003WR002086
2. Craig H. Isotopic Variations in Meteoric Waters. *Science.* 1961;133(3465):1702-1703. doi:10.1126/science.133.3465.1702
3. West JB, Bowen GJ, Dawson TE, Tu KP, eds. *Isoscapes*. Springer Netherlands; 2010. doi:10.1007/978-90-481-3354-3
4. Hobson KA, Wassenaar LI. *Tracking Animal Migration with Stable Isotopes*. Academic Press; 2008.
5. Soto DX, Wassenaar LI, Hobson KA. Stable hydrogen and oxygen isotopes in aquatic food webs are tracers of diet and provenance. *Funct Ecol.* 2013;27(2):535-543. doi:10.1111/1365-2435.12054
6. Fraser I, Meier-Augenstein W. Stable  $^2\text{H}$  isotope analysis of modern-day human hair and nails can aid forensic human identification. *Rapid Commun Mass Spectrom.* 2007;21(20):3279-3285. doi:10.1002/rcm.3209
7. Schellenberg A, Chmielus S, Schlicht C, et al. Multielement stable isotope ratios (H, C, N, S) of honey from different European regions. *Food Chem.* 2010;121(3):770-777. doi:10.1016/j.foodchem.2009.12.082
8. Chesson LA, Valenzuela LO, O'Grady SP, Cerling TE, Ehleringer JR. Hydrogen and Oxygen Stable Isotope Ratios of Milk in the United States. *J Agric Food Chem.* 2010;58(4):2358-2363. doi:10.1021/jf904151c
9. Chesson LA, Podlesak DW, Erkkila BR, Cerling TE, Ehleringer JR. Isotopic consequences of consumer food choice: Hydrogen and oxygen stable isotope ratios in

- 1  
2  
3 foods from fast food restaurants versus supermarkets. *Food Chem.* 2010;119(3):1250-  
4 1256. doi:10.1016/j.foodchem.2009.07.046  
5  
6  
7  
8  
9 10. Outram AK, Stear NA, Bendrey R, et al. The Earliest Horse Harnessing and Milking.  
10 *Science.* 2009;323(5919):1332-1335. doi:10.1126/science.1168594  
11  
12  
13  
14 11. Reynard LM, Hedges REM. Stable hydrogen isotopes of bone collagen in  
15 palaeodietary and palaeoenvironmental reconstruction. *J Archaeol Sci.*  
16 2008;35(7):1934-1942. doi:10.1016/j.jas.2007.12.004  
17  
18  
19  
20  
21 12. Sachse D, Billault I, Bowen GJ, et al. Molecular Paleohydrology: Interpreting the  
22 Hydrogen-Isotopic Composition of Lipid Biomarkers from Photosynthesizing  
23 Organisms. *Annu Rev Earth Planet Sci.* 2012;40(1):221-249. doi:10.1146/annurev-  
24 earth-042711-105535  
25  
26  
27  
28  
29  
30  
31 13. Schefuß E, Schouten S, Schneider RR. Climatic controls on central African hydrology  
32 during the past 20,000 years. *Nature.* 2005;437(7061):1003-1006.  
33 doi:10.1038/nature03945  
34  
35  
36  
37  
38 14. Tierney JE, Russell JM, Huang Y, Damsté JSS, Hopmans EC, Cohen AS. Northern  
39 Hemisphere Controls on Tropical Southeast African Climate During the Past 60,000  
40 Years. *Science.* 2008;322(5899):252-255. doi:10.1126/science.1160485  
41  
42  
43  
44  
45 15. Estep MF, Hoering TC. Biogeochemistry of the stable hydrogen isotopes. *Geochim*  
46 *Cosmochim Acta.* 1980;44(8):1197-1206. doi:10.1016/0016-7037(80)90073-3  
47  
48  
49  
50 16. da Silveira Lobo Sternberg L. D/H ratios of environmental water recorded by D/H ratios  
51 of plant lipids. *Nature.* 1988;333(6168):59-61. doi:10.1038/333059a0  
52  
53  
54  
55 17. Sessions AL. Review: Factors Controlling the Deuterium Contents of Sedimentary  
56 Hydrocarbons. *Org Geochem.* 2016;96:43-64. doi:10.1016/j.orggeochem.2016.02.012  
57  
58  
59  
60



- 1  
2  
3 18. Sessions AL, Sylva SP, Summons RE, Hayes JM. Isotopic exchange of carbon-bound  
4 hydrogen over geologic timescales. *Geochim Cosmochim Acta*. 2004;68(7):1545-1559.  
5  
6 doi:10.1016/j.gca.2003.06.004  
7  
8  
9  
10 19. Li C, Sessions AL, Kinnaman FS, Valentine DL. Hydrogen-isotopic variability in lipids  
11 from Santa Barbara Basin sediments. *Geochim Cosmochim Acta*. 2009;73(16):4803-  
12 4823. doi:10.1016/j.gca.2009.05.056  
13  
14  
15  
16  
17 20. Sauer PE, Eglinton TI, Hayes JM, Schimmelmann A, Sessions AL. Compound-specific  
18 D/H ratios of lipid biomarkers from sediments as a proxy for environmental and climatic  
19 conditions. *Geochim Cosmochim Acta*. 2001;65(2):213-222. doi:10.1016/S0016-  
20 7037(00)00520-2  
21  
22  
23  
24  
25  
26  
27 21. Sessions AL, Burgoyne TW, Schimmelmann A, Hayes JM. Fractionation of hydrogen  
28 isotopes in lipid biosynthesis. *Org Geochem*. 1999;30(9):1193-1200.  
29  
30 doi:10.1016/S0146-6380(99)00094-7  
31  
32  
33  
34 22. Smittenberg RH, Sachs JP. Purification of dinosterol for hydrogen isotopic analysis  
35 using high-performance liquid chromatography–mass spectrometry. *J Chromatogr A*.  
36 2007;1169(1-2):70-76. doi:10.1016/j.chroma.2007.09.018  
37  
38  
39  
40  
41 23. van der Meer MTJ, Baas M, Rijpstra WIC, et al. Hydrogen isotopic compositions of  
42 long-chain alkenones record freshwater flooding of the Eastern Mediterranean at the  
43 onset of sapropel deposition. *Earth Planet Sci Lett*. 2007;262(3-4):594-600.  
44  
45  
46  
47  
48  
49  
50  
51 24. Burgoyne TW, Hayes JM. Quantitative Production of H<sub>2</sub> by Pyrolysis of Gas  
52 Chromatographic Effluents. *Anal Chem*. 1998;70(24):5136-5141.  
53  
54  
55  
56  
57  
58  
59  
60

- 1  
2  
3  
4  
5  
6  
7  
8  
9  
10  
11  
12  
13  
14  
15  
16  
17  
18  
19  
20  
21  
22  
23  
24  
25  
26  
27  
28  
29  
30  
31  
32  
33  
34  
35  
36  
37  
38  
39  
40  
41  
42  
43  
44  
45  
46  
47  
48  
49  
50  
51  
52  
53  
54  
55  
56  
57  
58  
59  
60
25. Hilkert AW, Douthitt CB, Schlüter HJ, Brand WA. Isotope ratio monitoring gas chromatography/Mass spectrometry of D/H by high temperature conversion isotope ratio mass spectrometry. *Rapid Commun Mass Spectrom.* 1999;13(13):1226-1230. doi:10.1002/(SICI)1097-0231(19990715)13:13<1226::AID-RCM575>3.0.CO;2-9
  26. Scrimgeour CM, Begley IS, Thomason ML. Measurement of deuterium incorporation into fatty acids by gas chromatography/isotope ratio mass spectrometry. *Rapid Commun Mass Spectrom.* 1999;13(4):271-274. doi:10.1002/(SICI)1097-0231(19990228)13:4<271::AID-RCM468>3.0.CO;2-6
  27. Tobias HJ, Brenna JT. On-Line Pyrolysis as a Limitless Reduction Source for High-Precision Isotopic Analysis of Organic-Derived Hydrogen. *Anal Chem.* 1997;69(16):3148-3152. doi:10.1021/ac970332v
  28. Kaal E, Janssen H-G. Extending the molecular application range of gas chromatography. *J Chromatogr A.* 2008;1184(1-2):43-60. doi:10.1016/j.chroma.2007.11.114
  29. Bodlenner A, Liu W, Hirsch G, et al. C<sub>35</sub> Hopanoid Side Chain Biosynthesis: Reduction of Ribosylhopane into Bacteriohopanetetrol by a Cell-Free System from *Methylobacterium organophilum*. *ChemBioChem.* 2015;16(12):1764-1770. doi:10.1002/cbic.201500021
  30. Muhammad SA, Seow E-K, Omar AM, et al. Variation of delta H-2, delta O-18 & delta C-13 in crude palm oil from different regions in Malaysia: Potential of stable isotope signatures as a key traceability parameter. *Sci Justice.* 2018;58(1):59-66. doi:10.1016/j.scijus.2017.05.008
  31. Richter EK, Spangenberg JE, Kreuzer M, Leiber F. Characterization of Rapeseed (*Brassica napus*) Oils by Bulk C, O, H, and Fatty Acid C Stable Isotope Analyses. *J Agric Food Chem.* 2010;58(13):8048-8055. doi:10.1021/jf101128f

- 1  
2  
3 32. Spangenberg JE. Bulk C, H, O, and fatty acid C stable isotope analyses for purity  
4 assessment of vegetable oils from the southern and northern hemispheres. *Rapid*  
5 *Commun Mass Spectrom.* 2016;30(23):2447-2461. doi:10.1002/rcm.7734  
6  
7  
8  
9  
10  
11 33. Ehtesham E, Hayman AR, McComb KA, Van Hale R, Frew RD. Correlation of  
12 Geographical Location with Stable Isotope Values of Hydrogen and Carbon of Fatty  
13 Acids from New Zealand Milk and Bulk Milk Powder. *J Agric Food Chem.*  
14 2013;61(37):8914-8923. doi:10.1021/jf4024883  
15  
16  
17  
18  
19  
20 34. Paolini M, Bontempo L, Camin F. Compound-specific delta C-13 and delta H-2 analysis  
21 of olive oil fatty acids. *Talanta.* 2017;174:38-43. doi:10.1016/j.talanta.2017.05.080  
22  
23  
24  
25 35. Buchgraber M, Ulberth F, Anklam E. Cluster analysis for the systematic grouping of  
26 genuine cocoa butter and cocoa butter equivalent samples based on triglyceride  
27 patterns. *J Agric Food Chem.* 2004;52(12):3855-3860. doi:10.1021/jf035153v  
28  
29  
30  
31  
32 36. Fontecha J, Mayo I, Toledano G, Juárez M. Use of changes in triacylglycerols during  
33 ripening of cheeses with high lipolysis levels for detection of milk fat authenticity. *Int*  
34 *Dairy J.* 2006;16(12):1498-1504. doi:10.1016/j.idairyj.2005.12.005  
35  
36  
37  
38  
39  
40 37. Ruiz-Samblas C, Gonzalez-Casado A, Cuadros-Rodriguez L. Triacylglycerols  
41 Determination by High-temperature Gas Chromatography in the Analysis of Vegetable  
42 Oils and Foods: A Review of the Past 10 Years. *Crit Rev Food Sci Nutr.*  
43 2015;55(11):1618-1631. doi:10.1080/10408398.2012.713045  
44  
45  
46  
47  
48  
49 38. Pedentchouk N, Turich C. Carbon and hydrogen isotopic compositions of n-alkanes as  
50 a tool in petroleum exploration. *Geol Soc Lond Spec Publ.* 2018;468(1):105-125.  
51 doi:10.1144/SP468.1  
52  
53  
54  
55  
56  
57  
58  
59  
60

- 1  
2  
3 39. Radke J, Bechtel A, Gaupp R, et al. Correlation between hydrogen isotope ratios of  
4 lipid biomarkers and sediment maturity. *Geochim Cosmochim Acta*. 2005;69(23):5517-  
5 5530. doi:10.1016/j.gca.2005.07.014  
6  
7  
8  
9  
10 40. Li M, Huang Y, Obermajer M, Jiang C, Snowdon LR, Fowler MG. Hydrogen isotopic  
11 compositions of individual alkanes as a new approach to petroleum correlation: case  
12 studies from the Western Canada Sedimentary Basin. *Org Geochem*.  
13 2001;32(12):1387-1399. doi:10.1016/S0146-6380(01)00116-4  
14  
15  
16  
17  
18  
19 41. Schouten S, Hopmans EC, Sinninghe Damsté JS. The organic geochemistry of  
20 glycerol dialkyl glycerol tetraether lipids: A review. *Org Geochem*. 2013;54:19-61.  
21 doi:10.1016/j.orggeochem.2012.09.006  
22  
23  
24  
25  
26  
27 42. De Jonge C, Stadnitskaia A, Hopmans EC, Cherkashov G, Fedotov A, Sinninghe  
28 Damsté JS. In situ produced branched glycerol dialkyl glycerol tetraethers in  
29 suspended particulate matter from the Yenisei River, Eastern Siberia. *Geochim*  
30 *Cosmochim Acta*. 2014;125:476-491. doi:10.1016/j.gca.2013.10.031  
31  
32  
33  
34  
35  
36  
37 43. Peterse F, Kim J-H, Schouten S, Kristensen DK, Koç N, Sinninghe Damsté JS.  
38 Constraints on the application of the MBT/CBT palaeothermometer at high latitude  
39 environments (Svalbard, Norway). *Org Geochem*. 2009;40(6):692-699.  
40 doi:10.1016/j.orggeochem.2009.03.004  
41  
42  
43  
44  
45  
46 44. Wijker RS, Sessions AL, Fuhrer T, Phan M.  $^2\text{H}/^1\text{H}$  variation in microbial lipids is  
47 controlled by NADPH metabolism. *Proc Natl Acad Sci*. 2019;116(25):12173-12182.  
48 doi:10.1073/pnas.1818372116  
49  
50  
51  
52  
53 45. Correa-Ascencio M, Evershed RP. High throughput screening of organic residues in  
54 archaeological potsherds using direct acidified methanol extraction. *Anal Methods*.  
55 2014;6(5):1330-1340. doi:10.1039/C3AY41678J  
56  
57  
58  
59  
60

- 1  
2  
3 46. Kaneko M, Kitajima F, Naraoka H. Stable hydrogen isotope measurement of archaeal  
4 ether-bound hydrocarbons. *Org Geochem*. 2011;42(2):166-172.  
5  
6 doi:10.1016/j.orggeochem.2010.11.002  
7  
8  
9  
10 47. Lengger SK, Lipsewers YA, de Haas H, Sinninghe Damsté JS, Schouten S. Lack of  
11  
12 <sup>13</sup>C-label incorporation suggests low turnover rates of thaumarchaeal intact polar  
13  
14 tetraether lipids in sediments from the Iceland shelf. *Biogeosciences*. 2014;11(2):201-  
15  
16 216. doi:10.5194/bg-11-201-2014  
17  
18  
19  
20 48. Schouten S, Hoefs MJL, Koopmans MP, Bosch H-J, Sinninghe Damsté JS. Structural  
21  
22 characterization, occurrence and fate of archaeal ether-bound acyclic and cyclic  
23  
24 biphytanes and corresponding diols in sediments. *Org Geochem*. 1998;29(5-7):1305-  
25  
26 1319. doi:10.1016/S0146-6380(98)00131-4  
27  
28  
29  
30 49. Weber Y, Damsté JSS, Zopfi J, et al. Redox-dependent niche differentiation provides  
31  
32 evidence for multiple bacterial sources of glycerol tetraether lipids in lakes. *Proc Natl*  
33  
34 *Acad Sci*. 2018;115(43):10926-10931. doi:10.1073/pnas.1805186115  
35  
36  
37 50. Weber Y, De Jonge C, Rijpstra WIC, et al. Identification and carbon isotope  
38  
39 composition of a novel branched GDGT isomer in lake sediments: Evidence for  
40  
41 lacustrine branched GDGT production. *Geochim Cosmochim Acta*. 2015;154:118-129.  
42  
43 doi:10.1016/j.gca.2015.01.032  
44  
45  
46 51. Wegener G, Bausch M, Holler T, et al. Assessing sub-seafloor microbial activity by  
47  
48 combined stable isotope probing with deuterated water and <sup>13</sup>C-bicarbonate: Microbial  
49  
50 carbon assimilation in the sub-seafloor. *Environ Microbiol*. 2012;14(6):1517-1527.  
51  
52 doi:10.1111/j.1462-2920.2012.02739.x  
53  
54  
55 52. Weijers JWH, Wiesenberg GLB, Bol R, Hopmans EC, Pancost RD. Carbon isotopic  
56  
57 composition of branched tetraether membrane lipids in soils suggest a rapid turnover  
58  
59  
60

- 1  
2  
3 and a heterotrophic life style of their source organism(s). *Biogeosciences*.  
4  
5 2010;7(9):2959-2973. doi:10.5194/bg-7-2959-2010  
6  
7  
8  
9 53. Lengger SK, Sutton PA, Rowland SJ, et al. Archaeal and bacterial glycerol dialkyl  
10 glycerol tetraether (GDGT) lipids in environmental samples by high temperature-gas  
11 chromatography with flame ionisation and time-of-flight mass spectrometry detection.  
12  
13 *Org Geochem*. 2018;121:10-21. doi:10.1016/j.orggeochem.2018.03.012  
14  
15  
16  
17  
18 54. Sutton PA, Rowland SJ. High temperature gas chromatography–time-of-flight-mass  
19 spectrometry (HTGC–ToF-MS) for high-boiling compounds. *J Chromatogr A*.  
20  
21 2012;1243:69-80. doi:10.1016/j.chroma.2012.04.044  
22  
23  
24  
25 55. Worthington P, Blum P, Perez-Pomares F, Elthon T. Large-Scale Cultivation of  
26 Acidophilic Hyperthermophiles for Recovery of Secreted Proteins. *Appl Env Microbiol*.  
27  
28 2003;69(1):252-257. doi:10.1128/AEM.69.1.252-257.2003  
29  
30  
31  
32 56. Weber Y, Damsté JSS, Hopmans EC, Lehmann MF, Niemann H. Incomplete recovery  
33 of intact polar glycerol dialkyl glycerol tetraethers from lacustrine suspended biomass.  
34  
35 *Limnol Oceanogr Methods*. 2017;15(9):782-793. doi:10.1002/lom3.10198  
36  
37  
38  
39  
40 57. Schouten S, Huguet C, Hopmans EC, Kienhuis MVM, Sinninghe Damsté JS. Analytical  
41 methodology for TEX<sub>86</sub> paleothermometry by High-Performance Liquid  
42 Chromatography/Atmospheric Pressure Chemical Ionization-Mass Spectrometry. *Anal*  
43  
44 *Chem*. 2007;79(7):2940-2944. doi:10.1021/ac062339v  
45  
46  
47  
48  
49 58. Smittenberg RH, Hopmans EC, Schouten S, Sinninghe Damsté JS. Rapid isolation of  
50 biomarkers for compound specific radiocarbon dating using high-performance liquid  
51 chromatography and flow injection analysis–atmospheric pressure chemical ionisation  
52 mass spectrometry. *J Chromatogr A*. 2002;978(1):129-140. doi:10.1016/S0021-  
53  
54 9673(02)01427-9  
55  
56  
57  
58  
59  
60

- 1  
2  
3 59. Patwardhan AP, Thompson DH. Efficient Synthesis of 40- and 48-Membered  
4  
5 Tetraether Macrocyclic Bisphosphocholines. *Org Lett.* 1999;1(2):241-244.  
6  
7 doi:10.1021/ol990567o  
8  
9
- 10 60. Sessions AL, Jahnke LL, Schimmelmann A, Hayes JM. Hydrogen isotope fractionation  
11  
12 in lipids of the methane-oxidizing bacterium *Methylococcus capsulatus*. *Geochim*  
13  
14 *Cosmochim Acta.* 2002;66(22):3955-3969. doi:10.1016/S0016-7037(02)00981-X  
15  
16  
17
- 18 61. Sessions AL. Isotope-ratio detection for gas chromatography. *J Sep Sci.*  
19  
20 2006;29(12):1946-1961. doi:10.1002/jssc.200600002  
21  
22
- 23 62. Chikaraishi Y, Naraoka H.  $\delta^{13}\text{C}$  and  $\delta\text{D}$  relationships among three n-alkyl compound  
24  
25 classes (n-alkanoic acid, n-alkane and n-alkanol) of terrestrial higher plants. *Org*  
26  
27 *Geochem.* 2007;38(2):198-215. doi:10.1016/j.orggeochem.2006.10.003  
28  
29
- 30 63. Blumenberg M, Seifert R, Reitner J, Pape T, Michaelis W. Membrane lipid patterns  
31  
32 typify distinct anaerobic methanotrophic consortia. *Proc Natl Acad Sci.*  
33  
34 2004;101(30):11111-11116. doi:10.1073/pnas.0401188101  
35  
36
- 37 64. Zhang Z, Sachs JP. Hydrogen isotope fractionation in freshwater algae: I. Variations  
38  
39 among lipids and species. *Org Geochem.* 2007;38(4):582-608.  
40  
41 doi:10.1016/j.orggeochem.2006.12.004  
42  
43  
44
- 45 65. Osburn MR, Dawson KS, Fogel ML, Sessions AL. Fractionation of Hydrogen Isotopes  
46  
47 by Sulfate- and Nitrate-Reducing Bacteria. *Front Microbiol.* 2016;7.  
48  
49 doi:10.3389/fmicb.2016.01166  
50  
51
- 52 66. Zhang X, Gillespie AL, Sessions AL. Large D/H variations in bacterial lipids reflect  
53  
54 central metabolic pathways. *Proc Natl Acad Sci.* 2009;106(31):12580-12586.  
55  
56 doi:10.1073/pnas.0903030106  
57  
58  
59  
60

- 1  
2  
3 67. Campbell BJ, Sessions AL, Fox DN, et al. Minimal Influence of [NiFe] Hydrogenase on  
4 Hydrogen Isotope Fractionation in H<sub>2</sub>-Oxidizing Cupriavidus necator. *Front Microbiol.*  
5 2017;8. doi:10.3389/fmicb.2017.01886  
6  
7  
8  
9  
10 68. Dawson KS, Osburn MR, Sessions AL, Orphan VJ. Metabolic associations with  
11 archaea drive shifts in hydrogen isotope fractionation in sulfate-reducing bacterial lipids  
12 in cocultures and methane seeps. *Geobiology*. 2015;13(5):462-477.  
13 doi:10.1111/gbi.12140  
14  
15  
16  
17  
18  
19 69. Leavitt WD, Murphy SJ-L, Lynd LR, Bradley AS. Hydrogen isotope composition of  
20 Thermoanaerobacterium saccharolyticum lipids: Comparing wild type with a nfn-  
21 transhydrogenase mutant. *Org Geochem*. 2017;113:239-241.  
22 doi:10.1016/j.orggeochem.2017.06.020  
23  
24  
25  
26  
27  
28  
29 70. Leavitt WD, Flynn TM, Suess MK, Bradley AS. Transhydrogenase and Growth  
30 Substrate Influence Lipid Hydrogen Isotope Ratios in Desulfovibrio alaskensis G20.  
31 *Front Microbiol*. 2016;07. doi:10.3389/fmicb.2016.00918  
32  
33  
34  
35  
36  
37 71. Sinninghe Damsté JS, Rijpstra WIC, Foesel BU, et al. An overview of the occurrence of  
38 ether- and ester-linked iso-diabolic acid membrane lipids in microbial cultures of the  
39 Acidobacteria: Implications for brGDGT paleoproxies for temperature and pH. *Org*  
40 *Geochem*. 2018;124:63-76. doi:10.1016/j.orggeochem.2018.07.006  
41  
42  
43  
44  
45  
46  
47  
48  
49  
50  
51  
52  
53  
54  
55  
56  
57  
58  
59  
60



**Figure captions.**

**Figure 1.** GC/P/IRMS chromatograms under HT conditions, different temperature ramps were applied to the different mixtures. Shown is a mixture of *n*-alkanes up to *n*-C<sub>30</sub> with known  $\delta^2\text{H}$  values (Indiana B3-standard, A), a mixture of long chain *n*-alkanes up to *n*-C<sub>60</sub> (B), triacylglycerides (C), and a sample from a Black Sea methane seep (D) with GDGT-2 and GDGT-3 standards shown as inserts, note that the small second peak in GDGT-2 was a contaminant introduced during analysis that did not affect the measurement.

**Figure 2.**  $\delta^2\text{H}$  values of purchased triacylglyceride standards and isolated GDGTs determined by HTEA/IRMS compared with values as determined by HTGC/P/IRMS; values and standard errors are given in Table 1.

**Figure 3.** Measured  $\delta^2\text{H}$  values compared to peak heights. A RMSE of the B3 mixture compared to peak heights of the minimum peak height in the mixture. B Difference  $\delta^2\text{H}$  values of TGs determined by HTGC/P/IRMS to values determined by HTEA/IRMS plotted vs peak height.

**Figure 4.**  $\delta^2\text{H}$  values of ether lipids determined from environmental samples. brGDGTs and GDGT-0 were extracted from a peat (triangles) and all other compounds derived from a methane seep (circles). Error bars represent standard deviations.

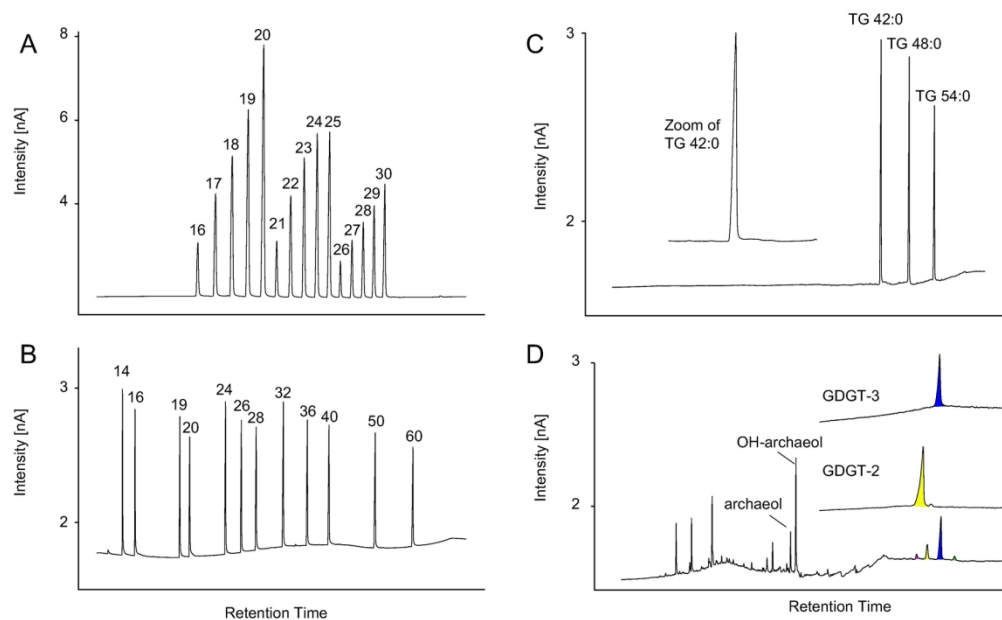


Figure 1. GC/P/IRMS chromatograms under HT conditions, different temperature ramps were applied to the different mixtures. Shown is a mixture of n-alkanes up to n-C30 with known  $\delta^2\text{H}$  values (Indiana B3-standard, A), a mixture of long chain n-alkanes up to n-C60 (B), triacylglycerides (C), and a sample from a Black Sea methane seep (D) with GDGT-2 and GDGT-3 standards shown as inserts, note that the small second peak in GDGT-2 was a contaminant introduced during analysis that did not affect the measurement.

162x120mm (300 x 300 DPI)

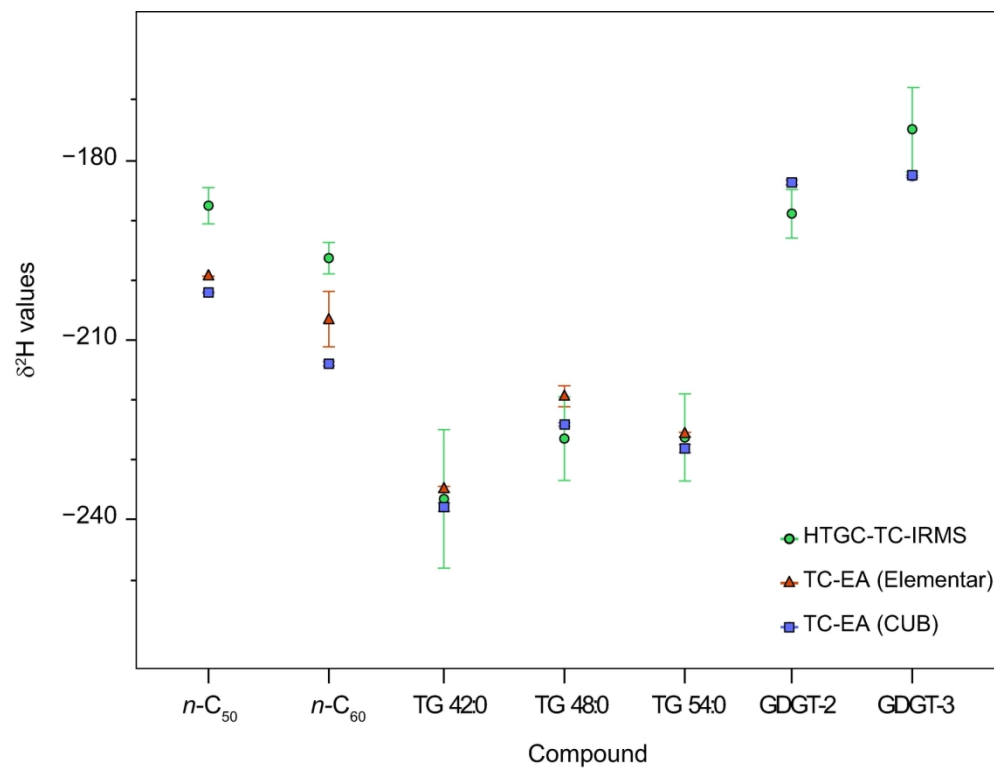


Figure 2.  $\delta^2\text{H}$  values of purchased triacylglyceride standards and isolated GDGTs determined by HTEA/IRMS compared with values as determined by HTGC/P/IRMS; values and standard errors are given in Table 1.

157x119mm (300 x 300 DPI)

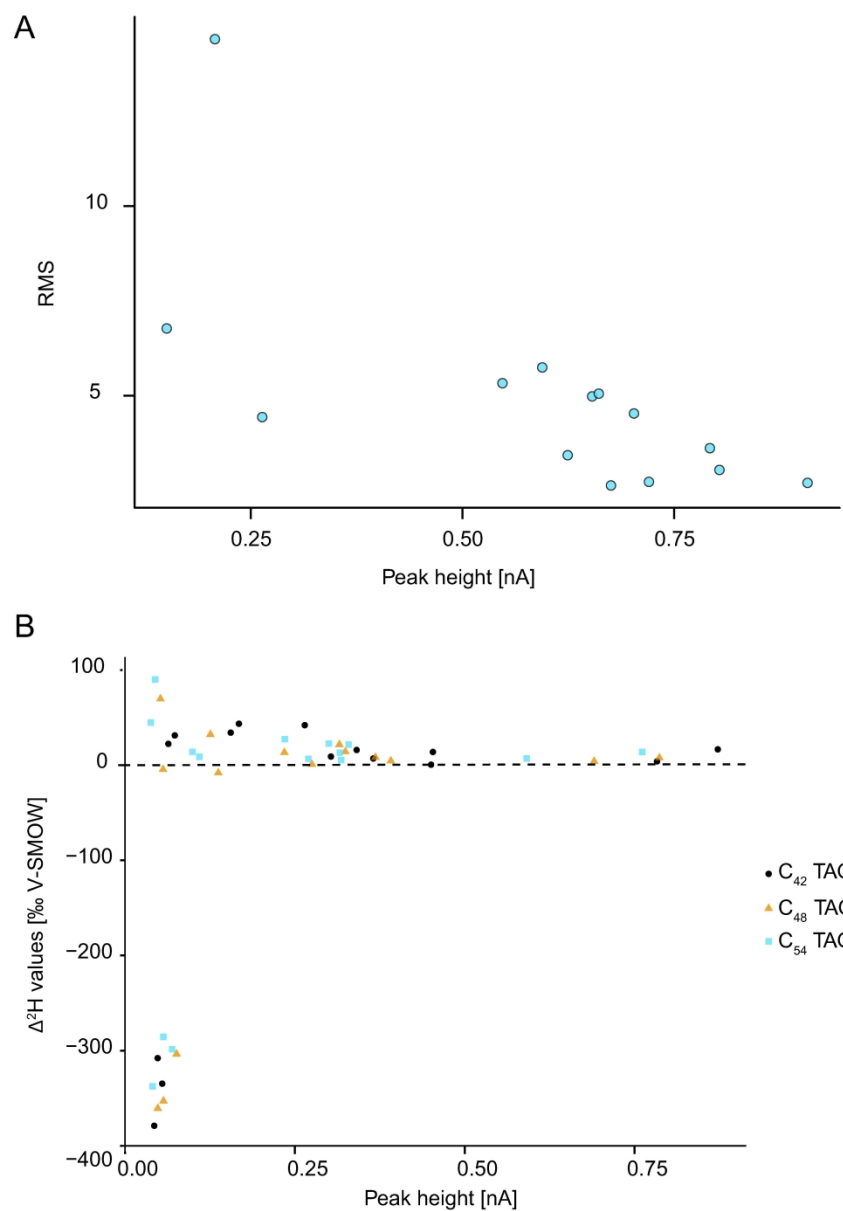


Figure 3. Measured  $\delta^2\text{H}$  values compared to peak heights. A RMSE of the B3 mixture compared to peak heights of the minimum peak height in the mixture. B Difference  $\delta^2\text{H}$  values of TGs determined by HTGC/P/IRMS to values determined by HTEA/IRMS plotted vs peak height.

168x240mm (600 x 600 DPI)

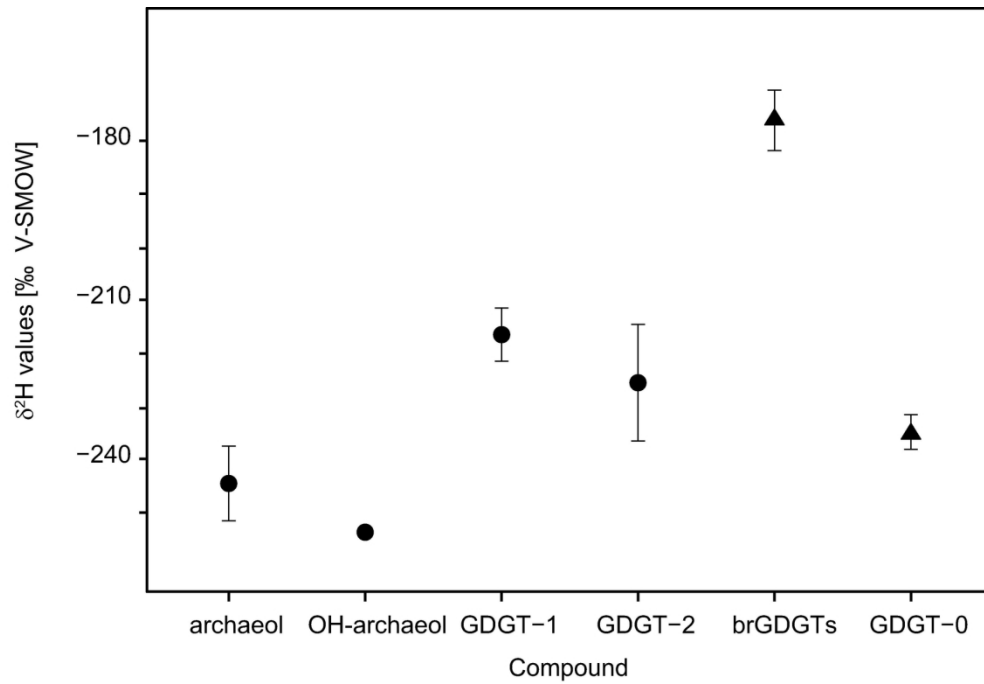


Figure 4.  $\delta^2\text{H}$  values of ether lipids determined from environmental samples. brGDGTs and GDGT-0 were extracted from a peat (triangles) and all other compounds derived from a methane seep (circles). Error bars represent standard deviations.

157x106mm (300 x 300 DPI)